





Article

# Pyrolysis Process as a Sustainable Management Option of Poultry Manure: Characterization of the Derived Biochars and Assessment of their Nutrient Release Capacities

Samar Hadroug <sup>1,2</sup>, Salah Jellali <sup>3,\*</sup> , James J. Leahy <sup>4</sup>, Marzena Kwapinska <sup>4</sup>, Mejdi Jeguirim <sup>5</sup> , Helmi Hamdi <sup>6</sup>  and Witold Kwapinski <sup>4</sup> 

<sup>1</sup> Wastewaters and Environment Laboratory, Water Research and Technologies Center, P.O. Box 273, Soliman 8020, Tunisia; samarhadroug@gmail.com

<sup>2</sup> National Agricultural Institute of Tunisia, University of Carthage, Tunis 1082, Tunisia

<sup>3</sup> Center for Environmental Studies and Research, Sultan Qaboos University, P.O. Box 31, Al-Khoud 123, Muscat, Oman

<sup>4</sup> Department of Chemical Sciences, Bernal Institute, University of Limerick, V94 T9PX Limerick, Ireland; j.j.leahy@ul.ie (J.J.L.); marzena.kwapinska@ul.ie (M.K.); witold.kwapinski@ul.ie (W.K.)

<sup>5</sup> CNRS, IS2M UMR 7361, University of Haute-Alsace, University of Strasbourg, F-68100 Mulhouse, France; mejdi.jeguirim@uha.fr

<sup>6</sup> Center for Sustainable Development, College of Arts and Sciences, Qatar University, P.O. Box 2713 Doha, Qatar; hhamdi@qu.edu.qa

\* Correspondence: s.jellali@squ.edu.om; Tel.: +968-2414-1807

Received: 10 September 2019; Accepted: 28 October 2019; Published: 30 October 2019



**Abstract:** Raw poultry manure (RPM) and its derived biochars at temperatures of 400 (B400) and 600 °C (B600) were physico-chemically characterized, and their ability to release nutrients was assessed under static conditions. The experimental results showed that RPM pyrolysis operation significantly affects its morphology, surface charges, and area, as well as its functional groups contents, which in turn influences its nutrient release ability. The batch experiments indicated that nutrient release from the RPM as well as biochars attains a pseudo-equilibrium state after a contact time of about 48 h. RPM pyrolysis increased phosphorus stability in residual biochars and, in contrast, transformed potassium to a more leachable form. For instance, at this contact time, P- and K-released amounts passed from 5.1 and 25.6 mg g<sup>-1</sup> for RPM to only 3.8 and more than 43.3 mg g<sup>-1</sup> for B400, respectively. On the other hand, six successive leaching batch experiments with a duration of 48 h each showed that P and K release from the produced biochars was a very slow process since negligible amounts continued to be released even after a total duration of 12 days. All these results suggest that RPM-derived biochars have specific physico-chemical characteristics allowing them to be used in agriculture as low-cost and slow-release fertilizers.

**Keywords:** raw poultry manure; pyrolysis; biochar; characterization; leaching; phosphorus; potassium

## 1. Introduction

Raw poultry manure (RPM) is a chicken waste that is produced from the normal operation of hatcheries, turkey, broiler, and egg laying [1]. Huge amounts of RPM are annually produced in the world. In the USA, the annual production of animal manure dry matter was estimated to be more than 19 million tons in 2018 [2]. In Tunisia, poultry production has seen a sharp increase during the last decade, generating about 400,000 tons/year of manure [3].

The composition of poultry manure is variable and depends mainly on the type of feed [4]. It generally contains high levels of organic carbon and nutrients, such as nitrogen, potassium, and phosphorus, which are indispensable macro-elements for soil fertility improvement and crop growth enhancement [5,6]. The sustainable management of this biowaste has been pointed out as an urgent priority due to its possible negative effects on human health and the environment [5,7]. In fact, the traditional methods for RPM management have various drawbacks [8]. Incineration has been the most widely used technique to reduce the huge volumes of RPM. However, the relatively high ash contents in RPM requires mitigation technologies [9]. Thermal gasification has also been investigated at the farm level, but gas quality is poor and requires extensive cleaning, which is expensive, particularly at the farm scale [10]. Likewise, the methane-fermentation process of malodorous RPM is generally limited by its excessive nitrogen contents [3]. Direct land application of fresh RPM or its composted form as organic amendments may result in: (i) The spread of pathogens [1], (ii) air pollution due to the emission of greenhouse gases and phytotoxic substances [11,12], and (iii) possible surface water resources eutrophication and groundwater pollution [3] due to nitrogen and phosphorus leaching [13]. One of the main potential methods used to reduce nutrient losses from RPM is thermal conversion by pyrolysis (in the absence of oxygen) into biogas and bio-oil that could have an important energetic added value [14–16] and a solid residue, named biochar. Biochars are highly porous carbonaceous materials that could be valorized for agricultural purposes as soil amendments [17,18], for climate change mitigation through carbon sequestration and a reduction of greenhouse gas emissions [19], and for environmental protection since they exhibit large capacities in removing various pollutants from both liquid and gas effluents [2,14,20,21]. All the above-cited effects are very dependent on the physico-chemical characteristics of the biochars that are mainly linked to the nature of the used feedstock and also to the pyrolysis experimental settings [22,23]. Therefore, in-depth characterization of produced biochars under given conditions has been pointed out as a key step in order to select the best method for their valorization [24]. On the other hand, according to our best of knowledge, no studies have investigated controlled RPM-derived biochars' capacities in releasing nutrients versus time by using the same biochars in successive leaching assays, which is close to what is happening in situ where biochar-amended soils are successively leached with rainfall and irrigation events. The majority of studies have attempted to monitor nutrient-release kinetics in a continuous way [22,24,25]. On the other hand, data on the relationships between the physico-chemical characteristics of RPM and RPM-derived biochars and their time-dependent capacity for phosphorus (P) and potassium (K) release in aqueous solutions are still missing.

Accordingly, the aims of the current research work were: (i) To study the thermal properties of RPM through thermogravimetric analyses, (ii) to determine the role of the selected pyrolysis temperatures on the physico-chemical properties of produced biochars, and (iii) to assess the importance of physico-chemical characteristics of RPM and its derived biochars on the kinetics and efficiency of phosphorus and potassium release under various experimental conditions.

## 2. Materials and Methods

### 2.1. Preparation of Raw Poultry Manure

The raw poultry manure was collected from a poultry farm in the city of Mornag (South of Tunis, Tunisia). Fresh RPM feedstock was first air-dried for about 10 days until a constant weight. Then, it was manually ground in order to have a relatively homogeneous particle size. Finally, RPM was mechanically sieved by using mechanical sieve shaker (Retch, Haan, Germany). Only fraction with a particle size less than 1 mm was collected and stored in bags for subsequent analysis.

### 2.2. Thermogravimetric Analysis of RPM

Thermogravimetric analysis (TGA) of RPM was performed using a thermal analyzer (LABSYS TG brand, Ireland) under the following thermo-analytical conditions: An RPM mass of 16.7 mg,

a heating gradient of  $10\text{ }^{\circ}\text{C min}^{-1}$  for temperatures varying from 30 to  $810\text{ }^{\circ}\text{C}$ , and a dynamic nitrogen atmosphere with a flow rate of  $10\text{ mL min}^{-1}$ . These TGA measurements were carried out in triplicate and the mean values are reported in this study. The TG curves giving the variation of the residual RPM mass (%) versus time/temperature were derived (DTG curves) in order to get a better idea about the kinetic of RPM mass losses ( $\text{mg min}^{-1}$ ) and to highlight even slight mass changes.

### 2.3. Biochar Production and Characterization

The biochars used in this study were derived from pyrolysis of air-dried RPM at two different temperatures (400 and  $600\text{ }^{\circ}\text{C}$ ). These biochars (named B400 and B600, consecutively) were produced using a laboratory pyrolysis furnace (Lenton brand oven) with dimensions of 67 cm length, 23 cm width, and 22 cm height. A pyrolysis metal container with a 13 cm length and 11 cm width equipped with four 0.5-cm holes in the lid was used, which permitted vapor elimination and maintained an air-absent environment in the container during the pyrolysis process. At the end of the pyrolysis operation, the container was taken out of the furnace and cooled down to room temperature. Solid residues (biochars) were removed from the container and placed in a plastic bag for use throughout this study.

Air-dried RPM, B400, and B600 were physically characterized through an assessment of: Particle size distribution by using a Malvern Mastersizer STD06 laser granulometry; surface area and pore volumes according to the Brunauer, Emmet, and Teller (BET) method, via the measurements obtained by  $\text{N}_2$  adsorption using an Autosorb Quantachrome apparatus; and finally, their morphology and structure through a scanning electron microscope (SEM) apparatus (SU-70). These solid matrices were also chemically characterized by the determination of: (i) Crystalline phase through X-ray diffraction (XRD) analyses; (ii) pH of zero-point charge (pHZC) according to the methodology given by Azzaz et al. [26]; (iii) elemental composition (C, H, N, O, S) by using a “vario EL cube” elemental analyzer; (iv) moisture, volatile matter, ash, and fixed carbon contents according to the British Standard Institution (BSI) protocol; and (v) their main contained functional groups through a Fourier transform infrared spectroscopy apparatus (Agilent Tech Cary 630, Ireland). The spectral resolution of the FTIR was  $1\text{ cm}^{-1}$  measured between 400 and  $4000\text{ cm}^{-1}$ .

### 2.4. Batch Nutrient Release Experiments

The batch experiments consisted of determining the P and K release kinetics from RPM and its derived biochars, as well as the effect of some key parameters, such as solution pH and solid matrices dosages, on this release process. These experiments were conducted at  $20 \pm 2\text{ }^{\circ}\text{C}$  in 120-mL capped flasks. During these assays, a defined amount of RPM or biochars was shaken in 50 mL of distilled water for a fixed time at 400 rpm using an IKA RT15 Power IKAMAG multi position magnetic stirrer for a contact time 48 h. Then, the resulting suspensions were centrifuged at 3000 rpm for 8 min using a ROTOFIX 32 apparatus and filtrated using a vacuum pumping system. Dissolved P and K concentrations in filtrates were analyzed by an inductively coupled plasma spectrometry (ICP) device (Agilent Tech 5100 ICP OES, Ireland). The released amount of P “ $q_P\text{ (mg g}^{-1}\text{)”$  or K “ $q_K\text{ (mg g}^{-1}\text)”$  per gram of solid matrix were determined as follows:

$$q_P = \frac{C_P}{D}, \quad (1)$$

$$q_K = \frac{C_K}{D}, \quad (2)$$

where  $C_P$ ,  $C_K$ , and  $D$  are the measured released concentrations of P and K, and the used solid matrix dose, respectively.

All the following batch nutrient release assays were carried out in triplicate and each analysis data reported in this study is an average of at least three independent parallel sample solutions.

#### 2.4.1. Effect of Contact Time

The kinetics of P and K release from RPM and the two derived biochars (B400 and B600) was monitored at 1, 5, 10, and 30 min and 4, 17, 24, and 48 h. During these assays, the solid matrices dosage, initial aqueous pH, and temperature were fixed to 10 g L<sup>-1</sup>, 5.6 (natural without adjustment), and 20 ± 2 °C, respectively. The subsequent nutrient release data were fitted to the most common models, namely pseudo-first order (PFO) and pseudo-second order (PSO) models. The corresponding equations and the related assumptions were given by Azzaz et al. [26]. In order to assess the applicability of these two models and their ability in fitting the current experimental data, average percentages errors (APEs) between the measured and calculated released amounts were estimated as follows [27]:

$$APE = \frac{\sum_{i=1}^N \left| \frac{q_{exp,i} - q_{th,i}}{q_{exp,i}} \right|}{N}, \quad (3)$$

where  $q_{exp,i}$  and  $q_{th,i}$  are the experimental and theoretical released P or K quantities at a given time “ $i$ ”, respectively.  $N$  is the number of experimental data.

#### 2.4.2. Effect of Initial Aqueous pH

The effect of initial aqueous pH on the rate of P and K release from RPM and the derived biochars was assessed for adjusted values of 3, 5.6 (natural pH), and 8. All these experiments were carried out at a constant dose of 10 g L<sup>-1</sup>, a temperature of 20 ± 2 °C, and a contact time of 48 h. The aqueous pH adjustment was performed by using 0.1 M HNO<sub>3</sub> or NaOH solutions.

#### 2.4.3. Effect of RPM and RPM-Derived Biochars Doses

The impact of RPM, B400, and B600 doses on P and K release was assessed for an initial aqueous pH of 5.6 (without adjustment), a temperature of 20 ± 2 °C and a contact time of 48 h. The tested doses were 2, 5, 10, and 15 g L<sup>-1</sup>.

#### 2.4.4. Successive Nutrient Release Experiments

In order to determine the slowness of the RPM and its two derived biochars' capacities in releasing P and K, six successive batch experiments were carried out for a total contact time duration of 12 days. For each leaching experiment, the same solid samples were put in contact with distilled water at a dose of 10 g L<sup>-1</sup>, an initial pH of 5.6 (without adjustment), and a contact time of 48 h. At the end of each assay, these solid matrices were recovered through filtration by using a vacuum pumping system with 0.45-µm paper filters, and then dried overnight at 40 °C. These dried samples were reused for the next leaching experiment in the presence of new distilled water under the same experimental conditions cited above.

### 2.5. Statistical Analysis

All the experimental data (except elemental analysis and granulometric distribution) for RPM and its derived biochars represent means of at least triplicate measurements. Data were analyzed using STATISTICA 8.0 (Statsoft, Tulsa, OK, USA). ANOVA with Duncan's multiple range test were applied for mean separation at  $p < 0.05$ .

## 3. Results and Discussion

### 3.1. Thermogravimetric Analysis of Raw Poultry Manure

The TG analysis of RPM was carried out under the experimental conditions given in Section 2.2. Figure 1 reports the RPM's TG records and the corresponding first derivative curve (DTG).

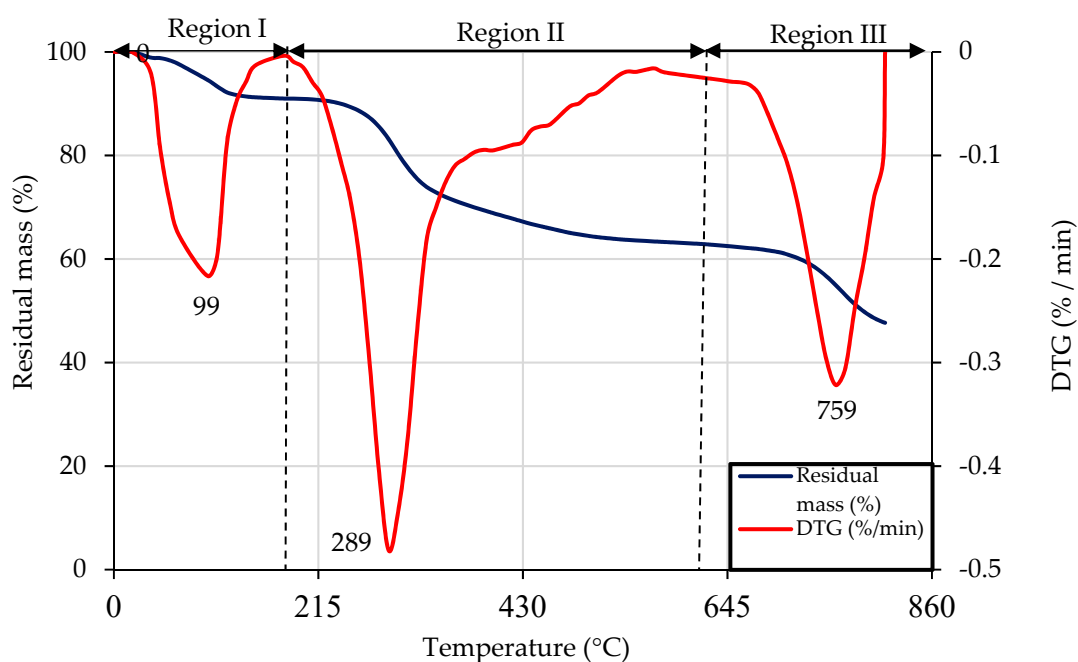


**Figure 1.** Thermograms (TGs) and its first derivative (DTG) of the used raw poultry manure (RPM dose = 16.7 mg; heating gradient =  $10\text{ }^{\circ}\text{C min}^{-1}$ ).

Figure 1 shows the presence of three regions with different thermal behavior. Region I spans a temperature interval of 49 to  $179\text{ }^{\circ}\text{C}$ , with a progressive mass loss reaching a maximum rate of 9% at the end of this interval. In this region, the maximum loss rate ( $0.22\% \text{ min}^{-1}$ ) was observed at a temperature of  $99\text{ }^{\circ}\text{C}$  and corresponds to moisture losses from the RPM. The second region is comprised between  $179$  and  $609\text{ }^{\circ}\text{C}$ , with a corresponding mass loss of about 27%. A maximum peak rate ( $0.48\% \text{ min}^{-1}$ ) was observed at a temperature of  $289\text{ }^{\circ}\text{C}$ . This peak apparition is mainly due to the thermo-oxidative degradation of highly oxygenated organic matter contained in RPM, such as labile alkyl systems, carbohydrates, and fatty acids [28,29]. The last thermal region corresponds to temperatures ranging between  $609$  to  $810\text{ }^{\circ}\text{C}$ , with a corresponding mass loss of 15%. A peak degradation rate was observed at a temperature of  $759\text{ }^{\circ}\text{C}$  ( $0.32\% \text{ min}^{-1}$ ) and could be attributed to the oxidation of mineral and biogenic salts, such as calcium and potassium carbonate [30]. A global similar trend was reported by Cimo et al. [30] when studying the thermal behavior of RPM collected from a Sicilian chicken farm in Italy. It is important to underline that P speciation in biochars is very dependent on the pyrolysis temperature. At low temperatures, the organic carbon compounds are aromatic and therefore do not overlap with the P vibrations. For biochars produced at higher temperatures, prevailing P forms are tricalcium phosphate, hydroxyapatite, calcium, and iron phosphate precipitates [31].

### 3.2. Characterization of Raw Poultry Manure and Biochars

The main physico-chemical properties of RPM as well as its two derived biochars at temperatures of  $400$  and  $600\text{ }^{\circ}\text{C}$  are given in Table 1. Granulometric characterization showed that the RPM and the corresponding biochars have a relatively fine texture with a mean particle size of  $0.48$ ,  $0.43$ , and  $0.31\text{ mm}$ , respectively. The uniformity coefficient (UC), which is the ratio of  $d_{60}/d_{10}$ , showed that RPM and B400 are heterogeneous media because their UCs are higher than 2. However, B600 could be considered as homogenous since its UC is lower than 2. The fine texture of the relative RPM and derived biochars indicates that they could play an important role in physico-chemical reactions with pollutants contained in rainwater or irrigation water [32].

**Table 1.** Main physico-chemical characteristics of raw poultry manure (RPM), B400, and B600 (\*: In Wt.% dry basis). For each parameter, means with the same lowercase letters are not statistically different at  $p < 0.05$ .

Physico-Chemical Property	RPM	B400	B600
Grains Size Distribution			
d <sub>10</sub> (mm)	0.21	0.16	0.19
d <sub>50</sub> (mm)	0.48	0.43	0.31
d <sub>60</sub> (mm)	0.57	0.44	0.33
Uniformity coefficient (UC = d <sub>60</sub> /d <sub>10</sub> )	2.71	2.75	1.74
Surface area (m <sup>2</sup> g <sup>-1</sup> )			
BET	0.88	4.30	5.34
Charges density			
pHZC	9.09 ± 0.03 a	10.87 ± 0.008 b	11.47 ± 0.015 c
Ultimate Analysis (%)*			
C	25.56 ± 1.39 b	22.04 ± 1.75 ab	21.22 2.30a
H	3.27 ± 0.79 b	0.87 ± 0.015 a	0.54 ± 0.04 a
N	2.19 ± 0.17 b	0.95 ± 0.19 a	0.64 ± 0.11 a
S	0.69 ± 0.017 a	0.68 ± 0.46 a	0.66 ± 0.005 a
O	69.35 ± 2.43 a	75.45 ± 2.31 b	76.90 ± 2.38 b
C/H	6.87 ± 1.85 a	25.33 ± 1.59 b	35.53 ± 7.61 c
Mineral Composition (mg g <sup>-1</sup> )			
Al	15.97	18.30	23.22
Fe	2.24	3.46	3.68
K	38.12	71.95	66.23
Mg	4.62	6.64	7.11
Na	18.98	20.17	28.67
P	17.00	20.33	43.17
Si	265.81	277.85	390.95
Ti	0.37	0.39	0.51
Proximate Analysis (%)*			
Moisture	16.69 ± 0.04 b	0.76 ± 0.09 a	0.80 ± 0.04 a
Ash	51.35 ± 0.38 a	78.64 ± 0.62 b	79.74 ± 0.18 c
Volatile matter	36.34 ± 0.18 b	4.08 ± 0.12 a	3.95 ± 0.13 a
Fixed carbon	11.99 ± 0.05 a	17.72 ± 0.13 c	16.18 ± 0.24 b

The BET surface area of RPM was assessed as 0.88 m<sup>2</sup> g<sup>-1</sup>. Pyrolysis operation increased this value to 4.30 and 5.34 m<sup>2</sup> g<sup>-1</sup> for B400 and B600, respectively (Table 1). These relatively low surface areas could be imputed to the existence of inorganic ash materials at high concentrations that might fill or block access to micropores [22,33]. Generally, higher specific surfaces areas are obtained for higher carbonization temperatures of biomasses [23,24]. It is worth mentioning that the BET surface areas of biochars significantly affect not only the subsurface contaminant mobility but also the microbial activities [22,29]. These authors reported that the BET specific surface areas of their RPM and derived biochar at 400 °C were 0.90 and 3.94 m<sup>2</sup> g<sup>-1</sup>, respectively, which are fairly close to the values found in the current study.

SEM analyses of the RPM and its derived biochars produced at temperatures of 400 and 600 °C are shown in Figure S1. RPM particles present a rough structure with a relatively oval shape (Figure S1). Besides, the pyrolysis process did not induce significant morphological changes. The presence of relatively small-sized particles in the three used solid materials (Figure S1) should play an important role in the nature of the physicochemical reactions with dissolved substances in liquid effluents [34].

The XRD spectra of RMP, B400, and B600 are given in Figure S2. Raw poultry manure showed an elevated background between  $2\theta = 21^\circ$ , likely attributable to the organic matter content [35,36]. The peaks at  $2\theta = 28.9^\circ$  and  $2\theta = 29.6^\circ$  indicate the presence of low crystallinity (quartz and calcite)



that already exists with a low intensity compared to its two biochars produced at 400 and 600 °C, respectively [37]. In addition to quartz and calcite, the sylvite (KCl), which is a cubic mesh mineral species of the chloride family, is present for B400 and B600 at peaks equal to  $2\theta = 40.5^\circ$ . The phosphate mineral whitlockite ((Ca,Mg)<sub>3</sub>(PO<sub>4</sub>)<sub>2</sub>) was identified only in B600 at a peak equal to  $2\theta = 47.3^\circ$  since phosphorus reached a more stable form [24,35].

The measured pHZC values of RPM, B400, and B600 were 9.09, 10.87, and 11.47, respectively (Table 1). This significant increase is mainly attributed to the concentration of the non-carbonized inorganic elements that were already present in the original feedstock [38]. The same behavior was reported by Song and Guo [22], who found that RPM carbonization at temperatures of 400 and 600 °C increased pHZC from 9.5 to 10.1 and 11.5, respectively. This observed alkaline property implies that these materials could be used as pH regulators for acidic soils when used as amendments or for acidic wastewaters when used as adsorbents for toxic substances. Such valorization pathways will significantly reduce the use of chemical reagents and hence the related expenses.

On the other hand, RPM pyrolysis significantly decreased C, H, N, and S contents as temperature increased (Table 1). For instance, original C, H, N, and S contents in RPM decreased respectively by 5.7%, 3.2%, 1.6%, and 0.02% in B600. These findings are mainly due to their transfer to bio-oil and/or incondensable exhaust during the pyrolysis process [24]. Furthermore, the C/H ratio increased with the increase of the pyrolysis temperature (Table 1) as a result of dehydration and decarboxylation reactions [33]. A similar trend was reported by Cimo et al. [30] when studying the pyrolysis of RPM collected from a chicken farm. They found C/H ratios of 7, 21, and 42 for RPM, and derived biochars at temperatures of 450 and 600 °C, respectively. The larger the C/H ratio is, the higher the polycondensation degree of organic systems. This confirms that an increasing pyrolysis temperature favors the formation of polycondensation aromatic rings.

The analysis of inorganic elements showed that silicon (Si), potassium (K), sodium (Na), phosphorus (P), aluminum (Al), and magnesium (Mg) exist in RPM with relatively high contents. The concentrations of these elements increase when increasing the pyrolysis temperature (Table 1). For instance, initial Mg, P, and K contents in RPM increased by 43.7% and 53.9%, 19.5% and 153.9%, 88.7% and 73.7% for B400 and B600, respectively. The presence of these nutrients in the produced biochars would be very useful for plant development and growth after land application.

Volatile matter (VM) contents significantly decreased from 36.3% for RPM to only 4.1% and 4.0% for B400 and B600. These changes are mainly due to the conversion of the RPM's organic matter into gaseous products during the pyrolysis process [39]. In contrast, ash contents increased from 51.4% for RPM to 78.6% and 79.7% for B400 and B600, respectively. The high ash contents of the three materials might be attributed to the physically incorporated soils and intrinsic inorganic elements, such as phosphorus and potassium, that are present in the raw manure and derived biochars [1]. Furthermore, the increase of the pyrolysis temperature leads to the dissociation of minerals from biomass [40]. As for ash, the fixed carbon contents increased after RPM pyrolysis, resulting in a more stable phase [39,41]. Unexpectedly, the measured fixed carbon content at 600 °C was slightly higher than the one measured at 400 °C (5.6%), which could be due to a combination of the samples' heterogeneity and analyses' uncertainties. Similar findings were reported by Enders et al. [42]. Finally, due to water evaporation during the pyrolysis process, the measured RPM moisture decreased from 16.7% to about 0.8% for both B400 and B600. Similar trends were also reported by Akdeniz and Novais et al. [2,37].

The FTIR spectra of raw manure feedstock and both biochars are given in Figure S3. For raw poultry manure, the major band near 3553 cm<sup>-1</sup> (H-bonded OH) was attributed to the stretching vibration of hydrogen bonds of carboxylic acid and alcohols [30]. Peaks at 2992 cm<sup>-1</sup> and 2865 cm<sup>-1</sup> revealed asymmetric and symmetric (–CH) stretching bands of CH<sub>3</sub> and CH<sub>2</sub> groups, respectively and are associated with the aliphatic functional groups existing in lipids [43]. The peak at 1650 cm<sup>-1</sup> concerns the C=O stretching of CO<sub>2</sub>H and C=O of primary amides, which indicates the presence of protein. A CH<sub>2</sub> deformation peak registered at 1416 cm<sup>-1</sup> is characteristic of saturated fatty acids and cellulose [44]. The peak at 1233 cm<sup>-1</sup> of C–O is associated with the stretching of carbohydrates. Finally,

the small peak appearing between 871 and 1024  $\text{cm}^{-1}$  in the raw feedstock was attributed to stretching -CH and represents the aromatic structures' out-of-plane bending vibrations [39].

The pyrolysis of RPM at 400 and 600 °C generated new transformational products. Compared to RPM, the spectra of produced biochars reveal the presence of higher aromatic and lower carbohydrates' structures. In this context, the intensity of the H-bonded OH peak significantly decreased with the increase of the pyrolysis temperature. This is likely related to the dehydration process during the pyrolysis operation and suggests that the carboxylic acid might be dissolved and hydrolyzed. Furthermore, the aliphatic C-H stretching of  $\text{CH}_3$  and  $\text{CH}_2$  groups observed respectively at 2992 and 2865  $\text{cm}^{-1}$  almost disappeared in the biochars' spectra, which could be imputed to the hydrolysis of aliphatic chain and dissolution. Similarly, the peak at 1650  $\text{cm}^{-1}$ , which is associated with C=O stretching of primary amides, presents a clear intensity decrease with an increasing pyrolysis temperature. This behavior is probably due to the decomposition of the C=O bonding that generally enhances the formation of monoxide carbon and dioxide carbon [43], and causes a change in N functional groups by pyrolysis [45,46]. The observed peak at 1416  $\text{cm}^{-1}$ , which is associated with  $\text{CH}_2$  deformation for both biochars, presents an intensity increase with temperature [39]. Also, the bonding of C-O increased at 1233  $\text{cm}^{-1}$ , which is associated with the stretching of -COH in alcohols and -COR in aliphatic ethers [44]. The peak between 871 and 1024  $\text{cm}^{-1}$  in the raw poultry manure is associated to aromatic -CH out-of-plane bending vibrations. This peak increased with the pyrolysis temperature, indicating a gradual conversion of aromatic structures during this process [44]. The presence of the various above-cited functional groups may play an important role in nutrient leaching from these biochars and especially pollutant adsorption from wastewaters [45,46]. For instance, P ion adsorption was confirmed by the apparition of a new P-O stretching vibration at 1050  $\text{cm}^{-1}$  [47].

### 3.3. Phosphorus and Potassium Release

The release of P and K from RPM and biochars was assessed in the batch mode under the various experimental conditions detailed in Section 2.4.

#### 3.3.1. Effect of Contact Time—Kinetic Release Study

In order to assess the effect of contact time on the release efficiency of P and K from RPM, B400, and B600, batch experiments were performed for an initial pH of 5.6 (without adjustment), a constant dose of 10  $\text{g L}^{-1}$ , and contact times varying between 1 min and 48 h (see Section 2.4.1). Outcomes indicated that P and K release from the three studied solid matrices was clearly a time-dependent process (Figure 2a,b and Figure 6a,b).

The P release kinetics were fast at the beginning of the experiment (until 4 h) as shown in Figure 2b. This is probably attributed to an ion exchange or desorption process and/or dissolution of some poorly crystalline or amorphous phosphates [25]. At this time, the released amount was estimated to 4.81  $\text{mg g}^{-1}$ , which represents 94% of the overall released quantity. Then, the released amount continued to increase but at much slower rates until an equilibrium state was reached. This latter state, which is characterized by an approximate released amount, was observed after approximately 17 h. A similar trend was also observed for potassium release (Figure 3a,b). The observed stiff slope at the beginning of the experiments indicates a quick and instantaneous release related to the abundance of low-energy-retained P or K (P/K) elements on the surface of the solid matrices. At this step, the release rate was relatively fast because P/K was essentially desorbed from the easily accessible sites to water located at the exterior surfaces of RPM and the derived biochars. When the release of P/K from the exterior surfaces reached its limits, P/K could be further released from the more inaccessible sites located at the inner surfaces of the tested materials.



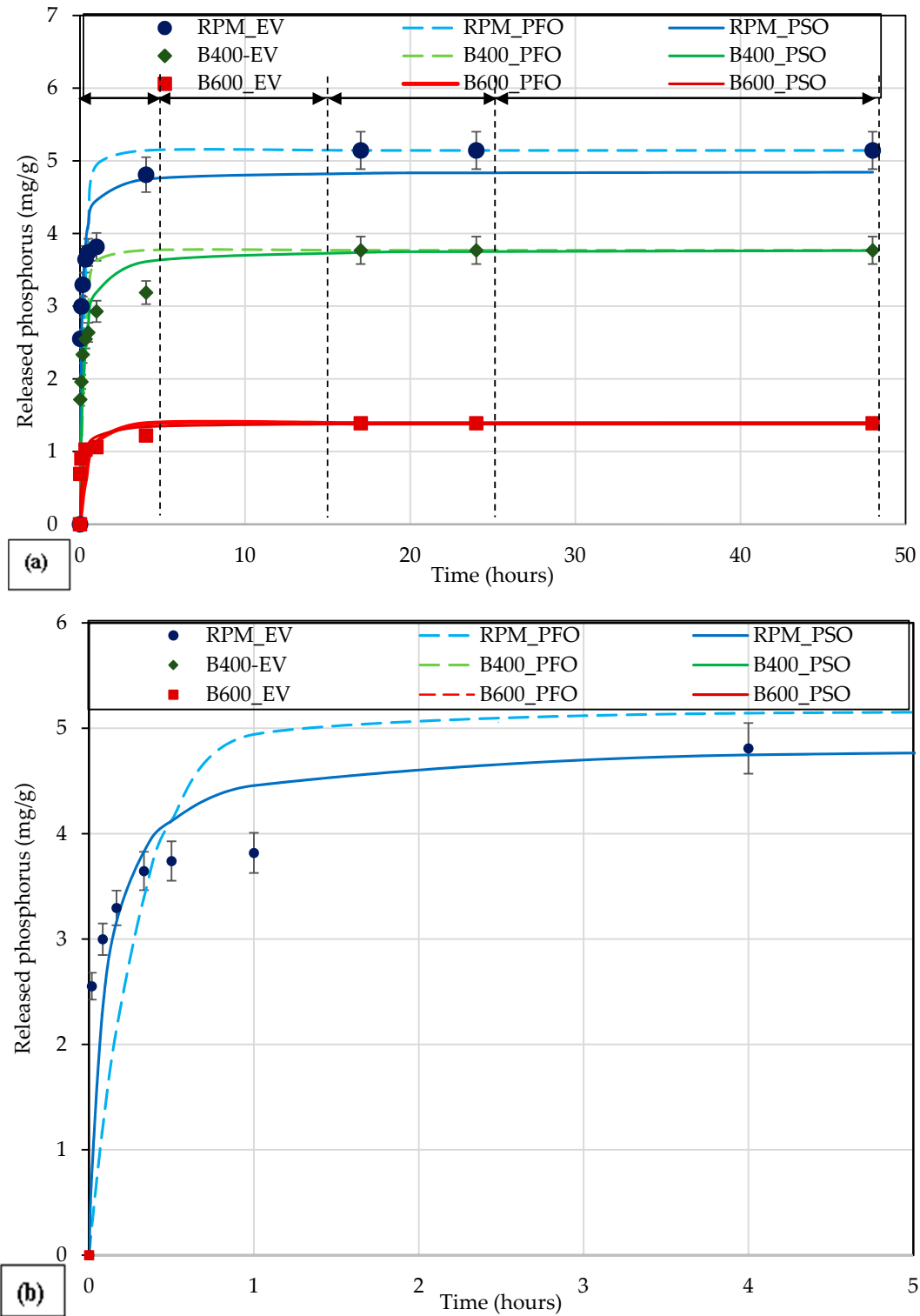


**Figure 2.** Comparison between the experimental quantities and theoretical ones of phosphorus released by raw poultry manure (RPM) and its derived biochars (EV: Experimental values; PFO: pseudo-first order; PSO: pseudo-second order) for 48 h (a) and zoom for 5 h (b).

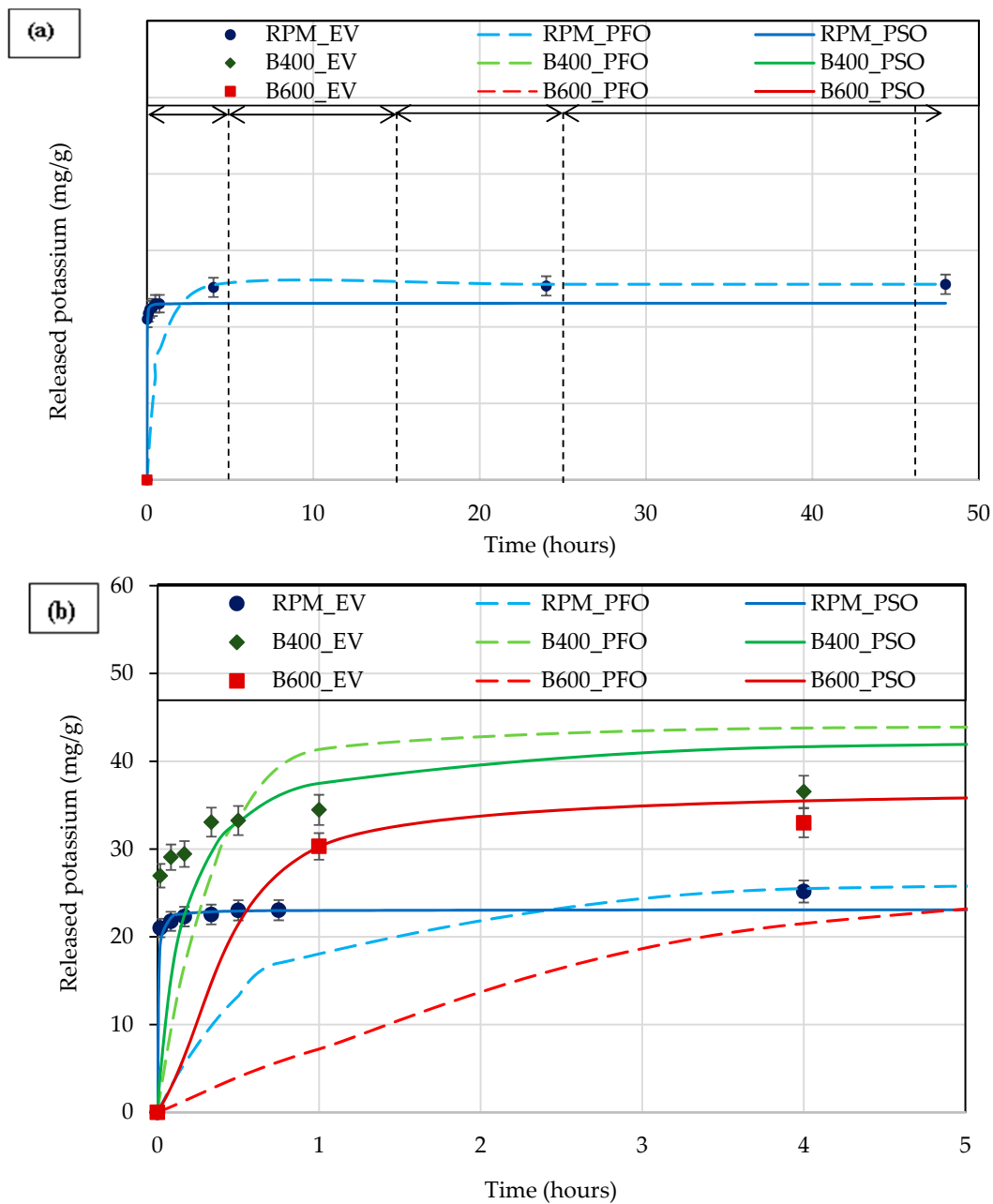


**Figure 3.** Comparison between the experimental and theoretical quantities of potassium released by raw poultry manure (RPM) and its derived biochars (EV: Experimental values; PFO: pseudo-first order; PSO: pseudo-second order) for 48 h (a) and zoom for 5 h (b).

Even if the pyrolysis process had concentrated P in the biochars compared to RPM (Table 1), at equilibrium, the released P amounts from RPM ( $5.14 \text{ mg g}^{-1}$ ) were much higher than those corresponding to B400 ( $3.77 \text{ mg g}^{-1}$ ) and B600 ( $1.39 \text{ mg g}^{-1}$ ). These amounts correspond to leachable P percentages of 30.2%, 18.5%, and 3.2% for RPM, B400, and B600, respectively. These rates are likely due to the fact that the pyrolysis process had converted a portion of RPM-containing phosphorus into water non-extractable forms, such as crystalline metal phosphates, which generally dissolve much more slowly and are less available [45,48]. In this context, Wang et al. [24] reported that RPM wastes collected from local hen houses (USA) released an average phosphorus amount of  $6.48 \text{ mg g}^{-1}$ . This quantity decreased to about  $1.04 \text{ mg g}^{-1}$  for its derived biochar at a temperature of  $600 \text{ }^{\circ}\text{C}$ . Similarly, Peak et al. [48] also reported that the released amount of phosphorus from an RPM sample (collected

from the region of Avila, Spain) was about 2.57 times higher than the one measured for its derived biochar produced at 500 °C.

The required time to attain an equilibrium state for K was much longer compared to P since it took about 48 h of contact time (Figure 3a). Furthermore, it appears that the pyrolysis process converted the initial potassium in RPM into a more leachable and water-soluble form in biochars through dissociation mechanisms [40]. As such, released K amounts were 25.6, 43.3, and 37.7 mg g<sup>-1</sup> for RPM, B400, and B600, respectively. Accordingly, Song and Guo [22] showed that the released potassium amount from an RPM-derived biochar at a temperature of 600 °C (44.61 mg g<sup>-1</sup>) was 1.9 higher than that observed for the raw biomass.

According to Tables 2 and 3, and Figures 2b and 3b, the confrontation of P/K release experimental data to those determined by the pseudo-first-order (PFO) and pseudo-second-order (PSO) models showed that the PFO model completely fails to reproduce the experimental values for the three tested solid materials. In fact, the calculated P/K determination coefficients as well as the related average percentage errors between the measured and the calculated values were not at all satisfactory. For instance, the “determination coefficients” and the APE of P were two by two 0.786 and 23.7%, 0.822 and 23.4%, and 0.734 and 29.6% for RPM, B400, and B600, respectively.

**Table 2.** Kinetic parameters of phosphorus release by RPM and its two derived biochars at 400 and 600 °C.

Solid Support	Pseudo-First-Order Model (PFO)			Pseudo-Second-Order Model (PSO)		
	K <sub>1,PFO</sub> (h <sup>-1</sup> )	R <sup>2</sup> <sub>PFO</sub>	APE <sub>PFO</sub> (%)	K <sub>2,PSO</sub> (g mg <sup>-1</sup> h <sup>-1</sup> )	R <sup>2</sup> <sub>PSO</sub>	APE <sub>PSO</sub> (%)
RPM	3.238	0.786	23.714	2.318	0.867	14.467
B400	3.242	0.822	23.431	1.435	0.879	17.766
B600	1.688	0.734	29.566	4.602	0.836	19.860

**Table 3.** Kinetic parameters of potassium release by RPM and its two derived biochars at 400 and 600 °C.

Solid Support	Pseudo-First-Order Model (PFO)			Pseudo-Second-Order Model (PSO)		
	K <sub>1,PFO</sub> (h <sup>-1</sup> )	R <sup>2</sup> <sub>PFO</sub>	APE <sub>PFO</sub> (%)	K <sub>2,PSO</sub> (g mg <sup>-1</sup> h <sup>-1</sup> )	R <sup>2</sup> <sub>PSO</sub>	APE <sub>PSO</sub> (%)
RPM	3.618	0.474	27.130	1.087	0.743	17.837
B400	2.886	0.668	26.199	0.150	0.750	19.517
B600	0.039	0.422	56.748	0.109	0.995	1.737

On the contrary, the PSO model succeeded to sufficiently reproduce the experimental data since the calculated determination coefficients (R<sup>2</sup>) for P or K were higher than that of the pseudo first order. Moreover, the calculated APE between the experimental and theoretical released P or K values were significantly lower than those calculated by the PFO model (Tables 2 and 3). For the three solid materials and the PSO model, the maximum values of APE for P and K were estimated at 19.9% (Table 2) and 19.5% (Table 3), respectively. However, the maximum values of this parameter were 29.6% and 56.7% for P and K, respectively. The highest non-accordance between the experimental and theoretical data corresponds to the initial phases of the experiments where the nutrient release slopes are maximal (Figures 2b and 3b). The fact that the experimental data were better fitted by the PSO suggests that nutrient leaching from RPM and its derived biochars might be controlled by a chemical process [26].

### 3.3.2. Effect of pH

The effect of initial aqueous pH on P and K release from the three materials was assessed under the experimental conditions described in Section 2.4.2. The results are illustrated in Figure 4a,b.

P-released amounts from RPM were approximately constant, with an average value of 5.51 mg g<sup>-1</sup>. However, for B400 and B600, P-released amounts increased with the increase of pH values. For instance, the released amount from B600 increased by about 43.5% when the pH increased from 3 to 8. Globally,

a similar variation trend was observed for K. The maximum released amount ( $41.33 \text{ mg g}^{-1}$ ) was observed for B400 at an initial aqueous leaching pH of 8. It is worth mentioning that high aqueous pH values could lead to the precipitation of the released phosphorus and potassium and therefore affect their availability to plants. For instance, depending on the aqueous pH value, phosphorus can exist as tricalcium phosphate, hydroxyapatite, calcium, and iron phosphates compounds [31]. However, it is very difficult for the precipitation of potassium as potassium hydroxide, which could be observed for very high pH values, to occur under the tested experimental conditions. It is important to underline that for high pH values, phosphorus could precipitate into calcium phosphate and magnesium phosphate, which makes P assimilation by crops more difficult [34,49]. These results confirmed that for a wide pH range, the biochars derived from RPM represent an important source of potassium that could be assimilated by various crops after soil application.

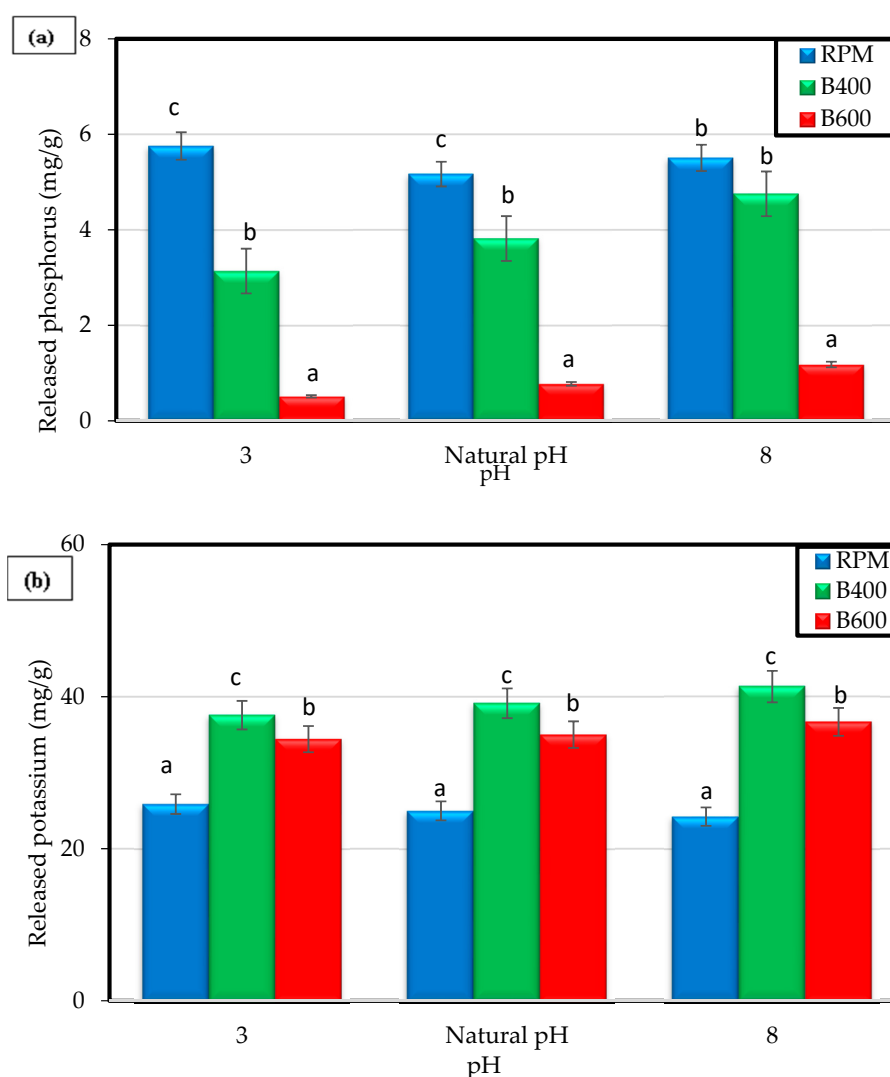


**Figure 4.** Effect of initial aqueous pH on the phosphorus (a) and potassium (b) release efficiency from raw poultry manure and its biochars derived at temperatures of 400 and 600 °C (dosage =  $10 \text{ g L}^{-1}$ ,  $T = 20 \pm 2 \text{ }^\circ\text{C}$ ). At each pH value, means with the same lowercase letters are not statistically different at  $p < 0.05$ .

### 3.3.3. Effect of Dose

The effect of RPM, B400, and B600 doses on P and K release efficiency was determined according to the experimental conditions given in Section 2.4.3 and are illustrated in Figure 5a,b.

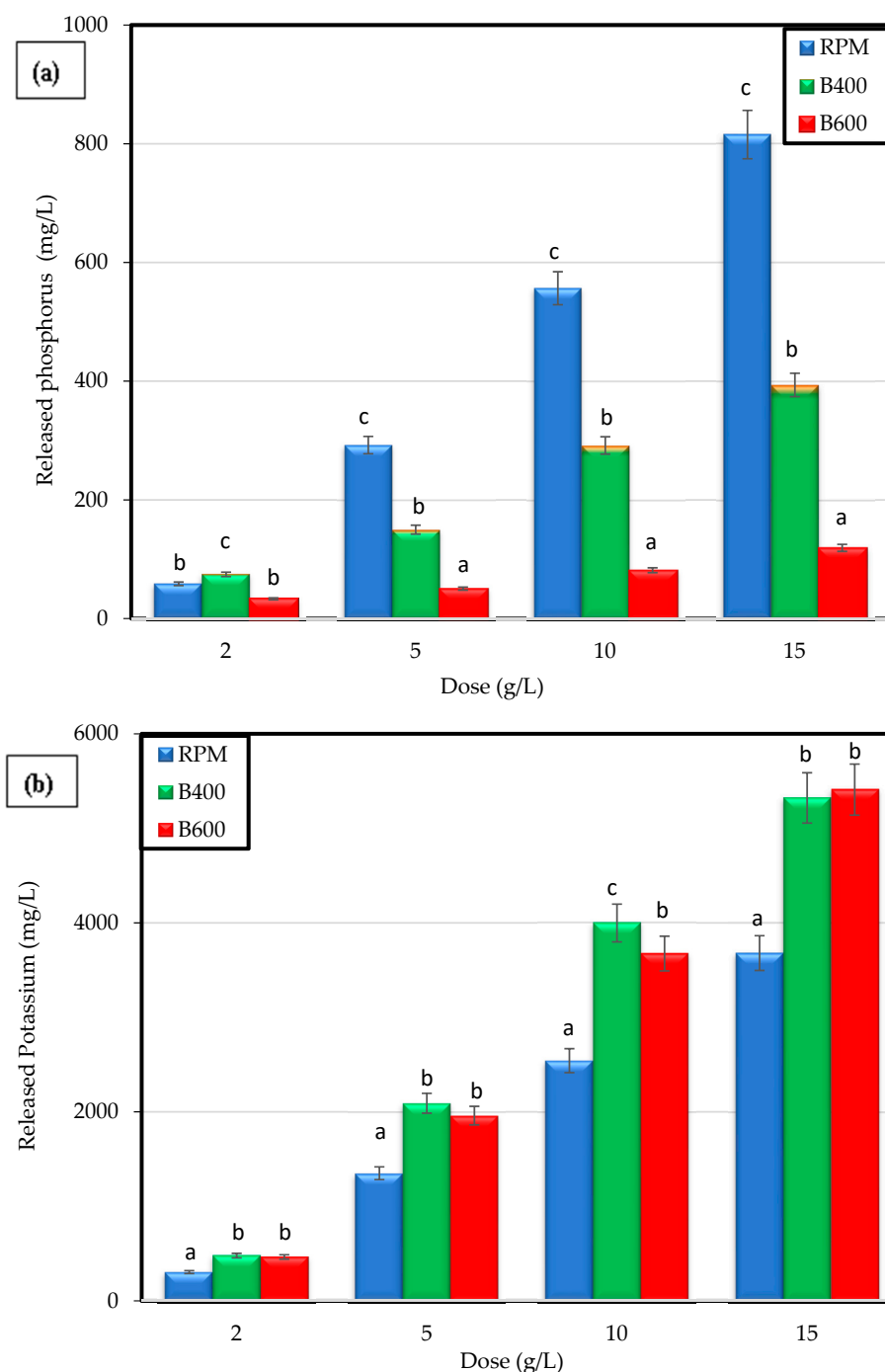


**Figure 5.** Effect of the used solid matrix doses on the release efficiency of phosphorus (a) and potassium (b) (pH = 6.2, T = 20 ± 2 °C). At each dose, means with the same lowercase letters are not statistically different at  $p < 0.05$ .

Released P or K concentrations increased significantly with the increase of the used dose. For example, P/K released concentrations increased from 58.58/304.83 to 815.47/3680.1 mg L<sup>-1</sup> for RPM, from 74.45/47.88 to 393.6/5321.8 mg L<sup>-1</sup> for B400, and from 33.18/464.7 to 119.13/5409.5 mg L<sup>-1</sup> for B600 when the material dose increased from 2 to 15 g L<sup>-1</sup>, respectively. This is mainly due to the increase of the available surface area of the solid matrices that could interact with the aqueous solutions [40]. Similar behavior was observed by Wang et al. [24] when studying the release of phosphorus from an RPM-derived biochar at 600 °C. They found that increasing the biochar concentration from 5 to 10 and then to 25 g L<sup>-1</sup> resulted in an increase of the released P from 8.8 to 14.0 and 26.8 mg L<sup>-1</sup>, respectively.

### 3.3.4. Successive Leaching Experiments—Nutrient Slow Release

The cumulative release of P and K from RPM, B400, and B600 for six successive leaching experiments (duration of 48 h for each one) is shown in Figure 6a,b, respectively.

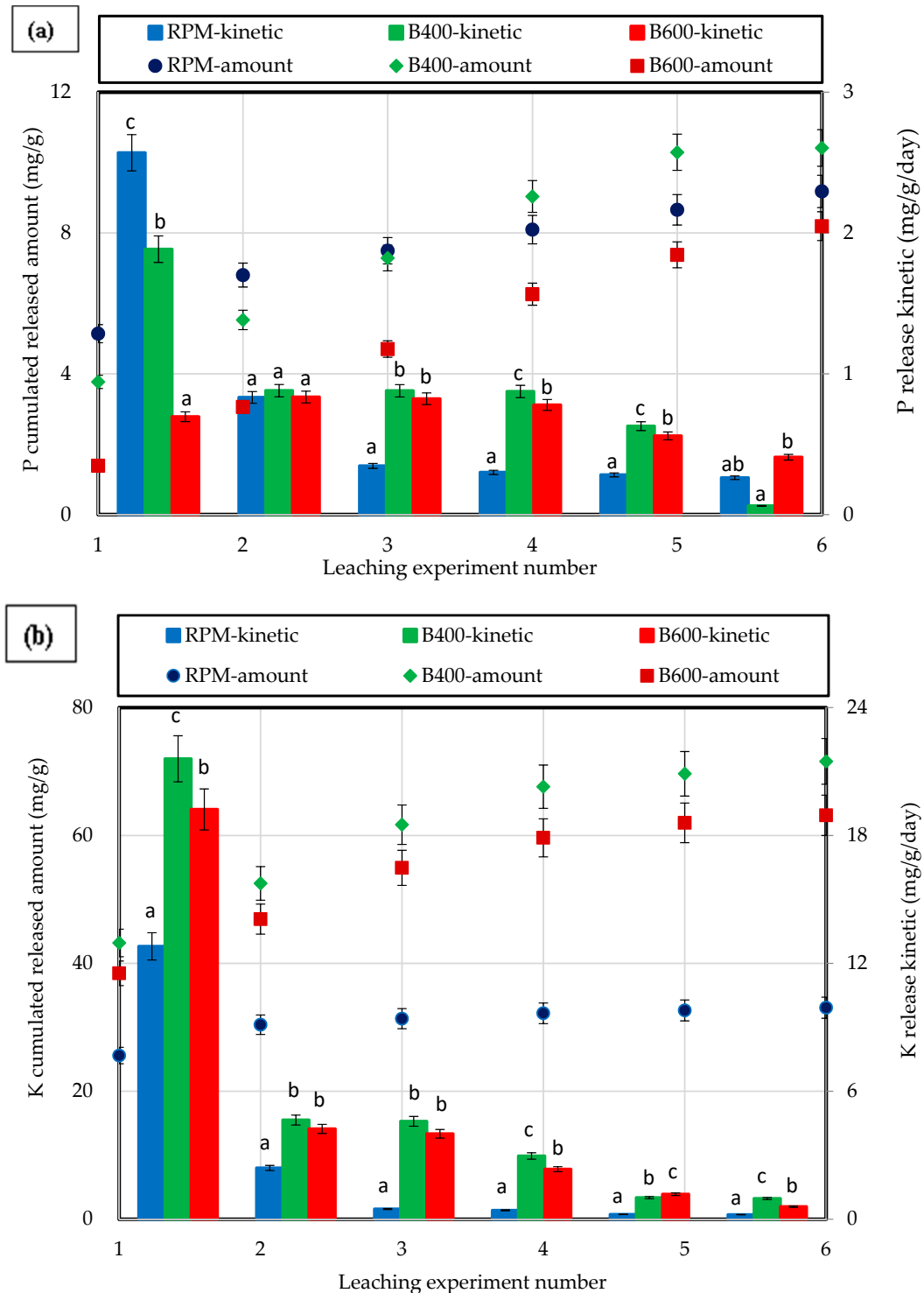


**Figure 6.** Effect of successive leaching experiments on the release of phosphorus (a) and potassium (b) from RPM and its two derived biochars: B400 and B600 (dosage = 10 g L<sup>-1</sup>; pH = 6.2; T = 20 ± 2 °C). At each leaching experiment number, means with the same lowercase letters are not statistically different at *p* < 0.05.



It can be clearly seen that for all the studied solid matrices, P release significantly increased with the operated number of leaching experiments. At the sixth assay, the maximal released amounts attained were approximately 9.2, 10.4, and 8.2 mg g<sup>-1</sup> for RPM, B400, and B600, respectively (Figure 6a), which are 78.7%, 176.3%, and 489.5% higher than those observed in the first leaching experiment. These released amounts correspond to 54.0%, 51.2%, and 19.0% of the initial contained P in RPM, B400, and B600, respectively (Table 1). These percentages are very important compared to the ones given in the scientific literature from continuous (not successive) leaching experiments. In fact, they were assessed as only 5.5% [24] and 6.2% [22] for RPM-derived biochars collected from broiler farms in Seaford (USA) at temperatures of 400 and 600 °C and contact times of 12 and 3 days, respectively. Besides, Liang et al. [25] estimated the P release percentage to be about 10% for a biochar derived from RPM collected from a Florida dairy farm at a temperature of 450 °C and a continuous contact time of 10 days.

Compared to the first leaching experiment, cumulated P amounts considerably increased at the sixth successive leaching assay by 78.7%, 176.3%, and 489.5% for RPM, B400, and B600, respectively (Figure 6a). Concerning the kinetic release, in contrast to RPM and the fourth leaching experiment, B400 and B600 continued to release P with relatively high average release kinetic rates of 0.878 and 0.812 mg g<sup>-1</sup> day<sup>-1</sup>. Even after the six successive leaching experiment (12 days), B400 and B600 were still releasing P at rates of 0.062 and 0.407 mg g<sup>-1</sup> day<sup>-1</sup>, respectively (Figure 6a).

Similar release trends were observed for potassium. For both B400 and B600 materials, released K amounts significantly increased with the progress of the leaching experiment, attaining values of 71.6 and 63.2 mg g<sup>-1</sup>, respectively, at the sixth leaching assay, corresponding to overall increase percentages of 65.7% and 64.3%, respectively, compared to the first leaching experiment (Figure 6b). These amounts represent 99.5% and 95.4% of the contained K in B400 and B600, respectively, confirming its transformation to a more leachable form and its slow release. These percentages were important when compared to continuous leaching assays where they were evaluated as only 45% to 49% for RPM-derived biochars collected from broiler farms in Seaford (USA) at temperatures varying between 400 and 600 °C, and a continuous contact time of 3 days [22].

Moreover, compared to RPM, until four successive leaching experiments, relatively high kinetic release rates of 4.071 and 3.531 mg g<sup>-1</sup> day<sup>-1</sup> were recorded for B400 and B600, respectively (Figure 6b). Even in the last leaching experiment, B400 and B600 were still releasing K at 0.968 and 0.587 mg g<sup>-1</sup> day<sup>-1</sup>, respectively (Figure 6b).

These outcomes indicate that the two RPM-derived biochars could be considered as slow-release fertilizers, where P and K could be available for several seasons in real conditions [50]. Unlike commercial fertilizers, where nutrient dissolution is very fast—even instantaneous for some products [51]—the use of RPM biochars as amendments for agricultural soils constitutes an important asset for both optimal plant growth and groundwater pollution reduction [52]. As crops also need nitrogen and other micronutrients, combining biochar application with chemical fertilizers or fresh composts has the benefits of simultaneously improving soil physical properties, nutrient retention, and plant yield [53].

#### 4. Conclusions

This research work demonstrated that raw poultry manure pyrolysis significantly affects its physico-chemical characteristics, especially the chemical composition, pH of zero-point charge, and surface properties, including the specific surface area and functional groups. Altogether, these characteristics play an important role on the nutrient release efficiency. Nevertheless, the chemical state of these nutrients in these solid matrices, which is very dependent on the used pyrolysis temperature, might be the most important factor influencing this process. The pyrolysis process favors P conversion into a more stable phase through its probable complexation with magnesium and/or calcium and therefore reduces its release rate in the aqueous phase. In contrast, RPM pyrolysis converts potassium into a more leachable form. On the other hand, compared to RPM, RPM-derived biochars

could be considered as an attractive soil conditioner with very slow nutrient release capacities. This promising property will result in a more efficient nutrient uptake by crops and limited leaching to both groundwater and surface runoff. Further investigation is currently being carried out to monitor the impact of biochar doses in agricultural soils under dynamic conditions on nutrient leaching ability and assimilation by selected plants.

**Supplementary Materials:** The following are available online at <http://www.mdpi.com/2073-4441/11/11/2271/s1>, Figure S1: SEM images of surface surfaces morphologies of RPM (a), B400 (b) and B600 (c), Figure S2: XRD images of crystalline phases of RPM, B400 and B600 (OM: organic matter; Q: quartz; C: calcite; S: sylvite and W: whitlockite), Figure S3: FTIR Spectra of RPM and its two derived biochars at temperatures of 400 and 600 °C.

**Author Contributions:** Conceptualization, S.H., S.J., W.K. and M.K.; methodology, S.H., S.J., J.J.L. and W.K.; software, H.H.; validation, S.J., W.K. and M.J.; formal analysis, S.H., M.J.; investigation, S.H., S.J. and W.K.; resources, M.K., J.J.L. and H.H.; data curation, S.H., S.J., M.J., H.H. and W.K.; writing—original draft preparation, S.H.; writing—review and editing, S.J., M.J., H.H. and W.K.; visualization, S.H., S.J. and W.K.; supervision, S.J. and W.K.; project administration, S.J. and W.K.; funding acquisition, S.J. and W.K.

**Funding:** This research was funded by the Tunisian Ministry of Higher Education and Scientific Research (MHESR). The scholarship covering the mobility fees of Ms S. Hadroug from CERTE, Tunisia to UL, Ireland was taken in charge by ERASMUS+ International Credit Mobility Programme.

**Acknowledgments:** This research work was carried out in close collaboration between CERTE (Tunisia) and the University of Limerick (Ireland) within the framework of the ERASMUS+ International Credit Mobility Programme. The authors would like to gratefully thank the financial contribution of this Programme and the Tunisian Ministry of Higher Education and Scientific Research.

**Conflicts of Interest:** The authors declare no conflict of interest.

## References

1. Mante, O.D.; Agblevor, F.A. Influence of pine wood shavings on the pyrolysis of poultry litter. *Waste Manag.* **2010**, *30*, 2537–2547. [[CrossRef](#)] [[PubMed](#)]
2. Akdeniz, N. A systematic review of biochar use in animal waste composting. *Waste Manag.* **2019**, *88*, 291–300. [[CrossRef](#)] [[PubMed](#)]
3. Sellami, F.; Jarboui, R.; Hachicha, S.; Medhioub, K.; Ammar, E. Co-composting of oil exhausted olive-cake, poultry manure and industrial residues of agro-food activity for soil amendment. *Bioresour. Technol.* **2008**, *99*, 1177–1188. [[CrossRef](#)] [[PubMed](#)]
4. Turan, N.G. The effects of natural zeolite on salinity level of poultry litter compost. *Bioresour. Technol.* **2008**, *99*, 2097–2101. [[CrossRef](#)] [[PubMed](#)]
5. Rodic, V.; Peric, L.; Djukic-Stojic, M.; Vukelic, N. The environmental impact of poultry production. *Biotechnol. Anim. Husb.* **2011**, *27*, 1673–1679. [[CrossRef](#)]
6. Lu, L.; Liao, X.D.; Luo, X.G. Nutritional strategies for reducing nitrogen, phosphorus and trace mineral excretions of livestock and poultry. *J. Integr. Agric.* **2017**, *16*, 2815–2833. [[CrossRef](#)]
7. Hu, Y.; Cheng, H.; Tao, S. Environmental and human health challenges of industrial livestock and poultry farming in China and their mitigation. *Environ. Int.* **2017**, *107*, 111–130. [[CrossRef](#)]
8. Cely, P.; Gascó, G.; Paz-Ferreiro, J.; Méndez, A. Agronomic properties of biochars from different manure wastes. *J. Anal. Appl. Pyrolysis* **2015**, *111*, 173–182. [[CrossRef](#)]
9. Lynch, D.; Henihan, A.M.; Kwapinski, W.; Zhang, L.; Leahy, J.J. Ash agglomeration and deposition during combustion of poultry litter in a bubbling fluidized-bed combustor. *Energy Fuels* **2013**, *27*, 4684–4694. [[CrossRef](#)]
10. Taupe, N.C.; Lynch, D.; Wnetrzak, R.; Kwapinska, M.; Kwapinski, W.; Leahy, J.J. Updraft gasification of poultry litter at farm-scale—A case study. *Waste Manag.* **2016**, *50*, 324–333. [[CrossRef](#)]
11. Kelleher, B.P.; O’Callaghan, M.N.; Leahy, M.J.; O’Dwyer, T.F.; Leahy, J.J. The use of fly ash from the combustion of poultry litter for the adsorption of chromium (III) from aqueous solution. *J. Chem. Technol. Biotechnol.* **2002**, *77*, 1212–1218. [[CrossRef](#)]
12. Agyarko-Mintah, E.; Cowie, A.; Singh, B.P.; Joseph, S.; Van Zwieten, L.; Cowie, A.; Harden, S.; Smillie, R. Biochar increases nitrogen retention and lowers greenhouse gas emissions when added to composting poultry litter. *Waste Manag.* **2017**, *61*, 138–149. [[CrossRef](#)] [[PubMed](#)]

13. Wongrod, S.; Simon, S.; Guibaud, G.; Lens, P.N.L.; Pechaud, Y.; Huguenot, D.; van Hullebusch, E.D. Lead sorption by biochar produced from digestates: Consequences of chemical modification and washing. *J. Environ. Manag.* **2018**, *219*, 277–284. [[CrossRef](#)]
14. Kwapinski, W.; Byrne, C.M.P.; Kryachko, E.; Wolfram, P.; Adley, C.; Leahy, J.J.; Novotny, E.H.; Hayes, M.H.B. Biochar from biomass and waste. *Waste Biomass Valoriz.* **2010**, *1*, 177–189. [[CrossRef](#)]
15. Mau, V.; Gross, A. Energy conversion and gas emissions from production and combustion of poultry-litter-derived hydrochar and biochar. *Appl. Energy* **2018**, *213*, 510–519. [[CrossRef](#)]
16. Hu, X.; Gholizadeh, M. Biomass Pyrolysis: A Review of the Process Development and Challenges from Initial Researches up to the Commercialisation Stage. *J. Energy Chem.* **2019**, 109–143. [[CrossRef](#)]
17. Ding, Y.; Liu, Y.; Liu, S.; Huang, X.; Li, Z.; Tan, X.; Zeng, G.; Zhou, L. Potential Benefits of Biochar in Agricultural Soils: A Review. *Pedosphere* **2017**, *27*, 645–661. [[CrossRef](#)]
18. Shashvatt, U.; Benoit, J.; Aris, H.; Blaney, L. CO<sub>2</sub>-assisted phosphorus extraction from poultry litter and selective recovery of struvite and potassium struvite. *Water Res.* **2018**, *143*, 19–27. [[CrossRef](#)]
19. Ghanim, B.M.; Pandey, D.S.; Kwapinski, W.; Leahy, J.J. Hydrothermal carbonisation of poultry litter: Effects of treatment temperature and residence time on yields and chemical properties of hydrochars. *Bioresour. Technol.* **2016**, *216*, 373–380. [[CrossRef](#)]
20. Azzaz, A.A.; Jellali, S.; Akrouf, H.; Assadi, A.A.; Bousselmi, L. Optimization of a cationic dye removal by a chemically modified agriculture by-product using response surface methodology: Biomasses characterization and adsorption properties. *Environ. Sci. Pollut. Res.* **2016**, *24*, 9831–9846. [[CrossRef](#)]
21. Abdallah, M.M.; Ahmad, M.N.; Walker, G.; Leahy, J.J.; Kwapinski, W. Batch and Continuous Systems for Zn, Cu, and Pb Metal Ions Adsorption on Spent Mushroom Compost Biochar. *Ind. Eng. Chem. Res.* **2019**, *58*, 7296–7307. [[CrossRef](#)]
22. Song, W.; Guo, M. Quality variations of poultry litter biochar generated at different pyrolysis temperatures. *J. Anal. Appl. Pyrolysis* **2012**, *94*, 138–145. [[CrossRef](#)]
23. Trazzi, P.A.; Leahy, J.J.; Hayes, M.H.B.; Kwapinski, W. Adsorption and desorption of phosphate on biochars. *J. Environ. Chem. Eng.* **2016**, *4*, 37–46. [[CrossRef](#)]
24. Wang, Y.; Lin, Y.; Chiu, P.C.; Imhoff, P.T.; Guo, M. Phosphorus release behaviors of poultry litter biochar as a soil amendment. *Sci. Total Environ.* **2015**, *512–513*, 454–463. [[CrossRef](#)] [[PubMed](#)]
25. Liang, Y.; Cao, X.; Zhao, L.; Xu, X.; Harris, W. Phosphorus Release from Dairy Manure, the Manure-Derived Biochar, and Their Amended Soil: Effects of Phosphorus Nature and Soil Property. *J. Environ. Qual.* **2014**, *43*, 1504–1509. [[CrossRef](#)]
26. Azzaz, A.A.; Jellali, S.; Assadi, A.A.; Bousselmi, L. Chemical treatment of orange tree sawdust for a cationic dye enhancement removal from aqueous solutions: Kinetic, equilibrium and thermodynamic studies. *Desalin. Water Treat.* **2016**, *57*, 22107–22119. [[CrossRef](#)]
27. Haddad, K.; Jellali, S.; Jeguirim, M.; Ben Hassen Trabelsi, A.; Limousy, L. Investigations on phosphorus recovery from aqueous solutions by biochars derived from magnesium-pretreated cypress sawdust. *J. Environ. Manag.* **2018**, *216*, 305–314. [[CrossRef](#)]
28. Xu, Y.; Chen, B. Investigation of thermodynamic parameters in the pyrolysis conversion of biomass and manure to biochars using thermogravimetric analysis. *Bioresour. Technol.* **2013**, *146*, 485–493. [[CrossRef](#)]
29. Zhao, L.; Cao, X.; Mašek, O.; Zimmerman, A. Heterogeneity of biochar properties as a function of feedstock sources and production temperatures. *J. Hazard. Mater.* **2013**, *256–257*, 1–9. [[CrossRef](#)]
30. Cimo, G.; Kucerik, J.; Berns, A.E.; Schaumann, G.E.; Alonzo, G.; Conte, P. Effect of Heating Time and Temperature on the Chemical Characteristics of Biochar from Poultry Manure. *J. Agric. Food Chem.* **2014**, *62*, 1912–1918. [[CrossRef](#)]
31. Bekiaris, G.; Peltre, C.; Jensen, L.S.; Bruun, S. Using FTIR-photoacoustic spectroscopy for phosphorus speciation analysis of biochars. *Spectrochim. Acta Part A Mol. Biomol. Spectrosc.* **2016**, *168*, 29–36. [[CrossRef](#)] [[PubMed](#)]
32. Kalderis, D.; Hawthorne, S.B.; Clifford, A.A.; Gidaracos, E. Interaction of soil, water and TNT during degradation of TNT on contaminated soil using subcritical water. *J. Hazard. Mater.* **2008**, *159*, 329–334. [[CrossRef](#)] [[PubMed](#)]
33. Jindo, K.; Mizumoto, H.; Sawada, Y.; Sanchez-Monedero, M.A.; Sonoki, T. Physical and chemical characterization of biochars derived from different agricultural residues. *Biogeosciences* **2014**, *11*, 6613–6621. [[CrossRef](#)]

34. Haddad, K.; Jellali, S.; Jaouadi, S.; Benlifa, M.; Mlayah, A.; Hamzaoui, A.H. Raw and treated marble wastes reuse as low cost materials for phosphorus removal from aqueous solutions: Efficiencies and mechanisms. *C. R. Chim.* **2015**, *18*, 75–87. [[CrossRef](#)]
35. Cao, X.; Harris, W. Properties of dairy-manure-derived biochar pertinent to its potential use in remediation. *Bioresour. Technol.* **2010**, *101*, 5222–5228. [[CrossRef](#)]
36. Wang, M.; Zhu, Y.; Cheng, L.; Anderson, B.; Zhao, X.; Wang, D.; Ding, A. ScienceDirect Review on utilization of biochar for metal-contaminated soil and sediment remediation. *J. Environ. Sci.* **2017**, *63*, 156–173. [[CrossRef](#)]
37. Novais, S.V.; Zenero, M.D.O.; Barreto, M.S.C.; Montes, C.R.; Cerri, C.E.P. Phosphorus removal from eutrophic water using modified biochar. *Sci. Total Environ.* **2018**, *633*, 825–835. [[CrossRef](#)]
38. Novak, J.M.; Busscher, W.J.; Laird, D.L.; Ahmedna, M.; Watts, D.W.; Niandou, M.A.S. Impact of Biochar Amendment on Fertility of a Southeastern Coastal Plain Soil. *Soil Sci.* **2009**, *174*, 105–112. [[CrossRef](#)]
39. Cantrell, K.B.; Hunt, P.G.; Uchimiya, M.; Novak, J.M.; Ro, K.S. Impact of pyrolysis temperature and manure source on physicochemical characteristics of biochar. *Bioresour. Technol.* **2012**, *107*, 419–428. [[CrossRef](#)]
40. Chen, X.; Lin, Q.; He, R.; Zhao, X.; Li, G. Hydrochar production from watermelon peel by hydrothermal carbonization. *Bioresour. Technol.* **2017**, *241*, 236–243. [[CrossRef](#)]
41. Domingues, R.R.; Trugilho, P.F.; Silva, C.A.; De Melo, I.C.N.A.; Melo, L.C.A.; Magriotis, Z.M.; Sánchez-Monedero, M.A. Properties of biochar derived from wood and high-nutrient biomasses with the aim of agronomic and environmental benefits. *PLoS ONE* **2017**, *12*, e0176884. [[CrossRef](#)] [[PubMed](#)]
42. Enders, A.; Hanley, K.; Whitman, T.; Joseph, S.; Lehmann, J. Characterization of biochars to evaluate recalcitrance and agronomic performance. *Bioresour. Technol.* **2012**, *114*, 644–653. [[CrossRef](#)] [[PubMed](#)]
43. Cao, W.; Cao, C.; Guo, L.; Jin, H.; Dargusch, M.; Bernhardt, D.; Yao, X. Hydrogen production from supercritical water gasification of chicken manure. *Int. J. Hydrogen Energy* **2016**, *41*, 22722–22731. [[CrossRef](#)]
44. Mau, V.; Quance, J.; Posmanik, R.; Gross, A. Phases' characteristics of poultry litter hydrothermal carbonization under a range of process parameters. *Bioresour. Technol.* **2016**, *219*, 632–642. [[CrossRef](#)] [[PubMed](#)]
45. Sun, J.; Hoon, S.; Jung, S.; Ryu, C.; Jeon, J.; Shin, M.; Park, Y. Production and utilization of biochar: A review. *J. Ind. Eng. Chem.* **2016**, *40*, 1–15.
46. Xiao, R.; Wang, J.J.; Gaston, L.A.; Zhou, B.; Park, J.H.; Li, R.; Dodla, S.K.; Zhang, Z. Biochar produced from mineral salt-impregnated chicken manure: Fertility properties and potential for carbon sequestration. *Waste Manag.* **2018**, *78*, 802–810. [[CrossRef](#)]
47. Halajnia, A.; Oustan, S.; Najafi, N.; Khataee, A.R.; Lakzian, A. Adsorption-desorption characteristics of nitrate, phosphate and sulfate on Mg-Al layered double hydroxide. *Appl. Clay Sci.* **2013**, *80–81*, 305–312. [[CrossRef](#)]
48. Peak, D.; Sims, J.T.; Sparks, D.L. Solid-state speciation of natural and alum-amended poultry litter using XANES spectroscopy. *Environ. Sci. Technol.* **2002**, *36*, 4253–4261. [[CrossRef](#)]
49. Barca, C.; Gérente, C.; Meyer, D.; Chazarenc, F.; Andrès, Y. Phosphate removal from synthetic and real wastewater using steel slags produced in Europe. *Water Res.* **2012**, *46*, 2376–2384. [[CrossRef](#)]
50. Mukherjee, A.; Zimmerman, A.R. Organic carbon and nutrient release from a range of laboratory-produced biochars and biochar-soil mixtures. *Geoderma* **2013**, *193*, 122–130. [[CrossRef](#)]
51. Liu, G.; Zotarelli, L.; Li, Y.; Dinkins, D.; Wang, Q. *Controlled-Release and Slow-Release Fertilizers as Nutrients Management Tools*; UF/IFAS Extension: Gainesville, FL, USA, 2017.
52. Sun, K.; Qiu, M.; Han, L.; Jin, J.; Wang, Z.; Pan, Z.; Xing, B. Speciation of phosphorus in plant- and manure-derived biochars and its dissolution under various aqueous conditions. *Sci. Total Environ.* **2018**, *634*, 1300–1307. [[CrossRef](#)] [[PubMed](#)]
53. Schulz, H.; Glaser, B. Effects of biochar compared to organic and inorganic fertilizers on soil quality and plant growth in a greenhouse experiment. *J. Plant Nutr. Soil Sci.* **2012**, *175*, 410–422. [[CrossRef](#)]

